ARCHIVES OF ELECTRICAL ENGINEERING VOL. 71(2), pp. 283–296 (2022)

DOI 10.24425/aee.2022.140711

A new topology of double-stator permanent magnet machine equipped with AC windings on both stators

CHUKWUEMEKA CHIJIOKE AWAH

Michael Okpara University of Agriculture
Umudike, Nigeria
e-mail: awahchukwuemeka@gmail.com

(Received: 29.09.2021, revised: 08.11.2021)

Abstract: A new double stator permanent magnet machine having two sets of alternating current (AC) windings in separate stators is proposed in this study. The proposed machine is appropriate for low-speed direct-drive applications. 2D- and 3D-finite element analysis (FEA) is adopted in the result predictions. The considered machine elements are: coil and phase flux linkage, coil and phase induced-electromotive force (EMF), copper loss, current density and torque characteristics. The analysis shows that the studied permanent magnet (PM) machine has better electromagnetic performance than its single-stator equivalent. Moreover, the proposed machine has potential for higher reliability if the separate stators are used independently. The effect of design parameters on open-circuit flux linkage and induced-electromotive force, as well as on the average electromagnetic torque of the proposed double stator machine is also presented. It is observed that for each of the investigated design variables, there is a need to select the optimal value in order to achieve the best average torque. The investigated design parameters are: the split ratio, magnet thickness, rotor radial thickness, inner stator tooth-width, rotor inner and outer iron-width/pitch ratio, and stator yoke size.

Key words: double and single stator, electromotive force, flux linkage, machine geometries, and torque

1. Introduction

Many different topologies of the double-stator permanent magnet (DSPM) machine are being investigated lately, due its advantages over the single stator permanent magnet machines of similar size. It is proved that DSPM machines have superior electromagnetic performance than their single-stator equivalents, as justified in [1] and [2]; though, these virtues are usually at

a higher cost consequence with increased machine structural complexity. Therefore, a new type of a high-performance double-stator permanent magnet machine having alternating current (AC) windings on both the inner and outer stators is proposed and compared in this present study, in order to obtain an improved overall machine performance.

Wang *et al*. (2011) in [3] proved that the output performance of a given double-stator PM machine is a function of its most favorable split or aspect ratio, in addition to its best stator and rotor pole selection feasibility. Moreover, the investigation in [3] reveals that there is an inverse relationship between the aspect ratio of the machine and its corresponding magnetic loading; hence, there is a need for a careful selection of these variables for optimum torque production and possible cost reduction. Further, the impact of the split ratio on the overall output torque of a given PM machine is reconfirmed in [4] and proved to be significant; the study also noted that thermal constraints would further deteriorate the output torque of a given electric machine, if not minimized. The proposed machine structure as well as the adopted 3D FEA mesh distribution diagram in this present study is depicted in Fig. 1, with its parametric dimensions listed in Table 1.

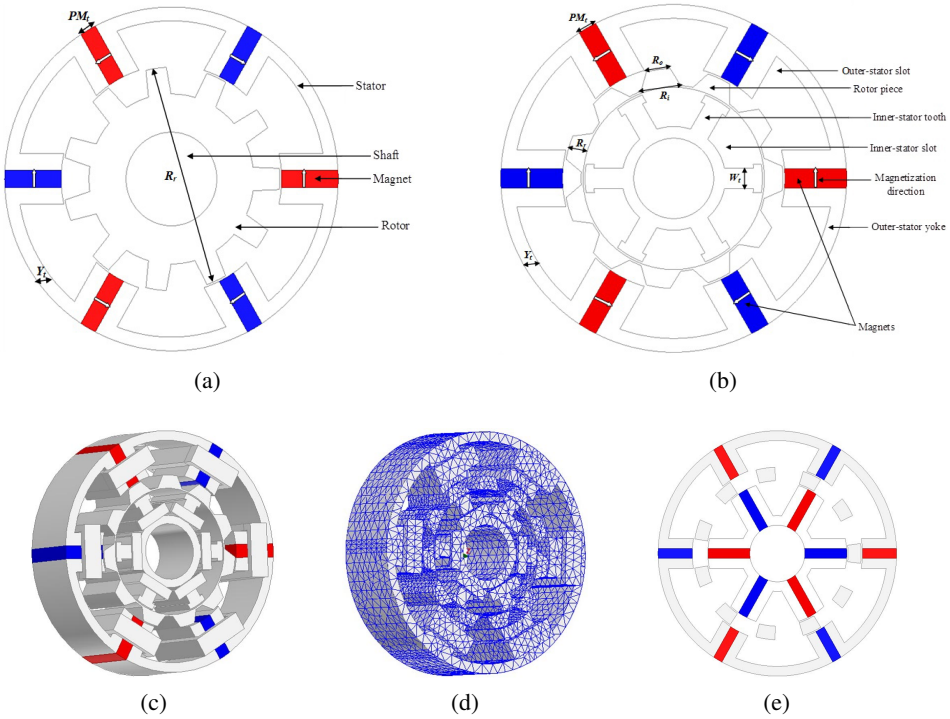

Fig. 1. Studied machines: conventional flux-switching permanent magnet machine (FSPM) [5] (a); proposed 2D FEA model (b); proposed 3D FEA model (c); 3D FEA mesh (d); dual stator FSPM [6] (e)

It is on record that when a permanent magnet machine is equipped with superconducting conductors, then it exhibits larger output torque than its counterpart that has traditional copper coils, as reported in [7]. However, the deployment of superconducting materials could increase the demagnetization potential of a PM machine; hence, an adequate structural architecture obtained

Table 1. Parameters of the compared machines, 2D FEA

Parameter name	**Symbol**	**Value**	**Unit**
Stator pole number	–	6	–
Rotor pole number	–	11	–
Air-gap length	–	0.5	mm
Stack length	–	25	mm
Machine outer radius	–	45	mm
Winding factor	–	0.6	–
Phase number of turns	–	72	–
PM remanence	Br	1.2	T
Coercivity	H	–909456.82	A/m

Comparison	**Conventional FSPM machine**			**Proposed DSPM machine**		
Parameter name	**Symbol**	**Value**	**Unit**	**Symbol**	**Value**	**Unit**
Split ratio or aspect ratio	S_r	0.65	–	S_r	0.638	–
Magnet width	PM_t	4.45	mm	PM_t	4.90	mm
Rotor radial thickness	R_r	29.25	mm	R_r	4.86	mm
Rotor inner iron-width/pitch ratio	R_i	N/A	mm	R_i	0.82	mm
Rotor outer iron-width/pitch ratio	R_o	N/A	mm	R_o	0.39	mm
Outer stator back-iron size	Y_t	3.60	mm	Y_t	3.57	mm
Inner stator back-iron size	–	N/A	mm	–	3.04	mm
Inner stator tooth-width	W_t	N/A	mm	W_t	5.17	mm
Peak-to-peak output torque at 30 W	–	3.78	Nm	–	4.29	Nm
Peak-to-peak cogging torque	–	0.28	Nm	–	0.08	Nm
Total loss at 400 rpm	–	18.73	W	–	13.13	W
Efficiency at 15 A		86.55	%		88.17	%

through geometric optimization is required to avoid this flaw, as established in [8]. Moreover, it should be noted that superconducting machines are characterized by high amount of losses as well as reduced reliability due to its structural arrangement. Nevertheless, a double-stator PM machine having superconducting coils which has improved reliability and enhanced output power compared to a conventional single-stator superconducting machine is presented in [9]. The investigation in [9] also reveals that a high level of decoupling between the different kinds of coils i.e. the superconducting coils and armature coils exists in such a machine, in addition to an inherent ability to reduce the adverse properties owing to armature reaction and of course with a value-added heat dissipation facility.

The studies in [10] and [11] demonstrate the structural geometric design variables of a flux-switching permanent magnet machine; however, a good consideration between these design variables and the resulting parasitic features such as cogging torque and total harmonic distortion (THD) is essential in yielding optimum machine performance. Meanwhile, the right stator pole and rotor pole combinations plus possible reduction in the machine's slot opening are recommended for better electromagnetic output. Also, [11] further revealed that an FSPM machine has lower cogging torque, lower THD and lower torque ripple compared to an equivalent surface-mounted PM machine; though, with relatively lower capacity to withstand overload in addition to lesser speed coverage. Furthermore, voltage harmonic effects on flux-switching PM machines could be ameliorated by using any of the following methods: splitting the machine's rotor tooth, rotor step skewing and rotor tooth tip modification; though, rotor step skewing is the most recommended, as established in [12].

In [13], Chen *et al*. (2017) developed a double-stator machine with dual excitation windings that is free of PMs, whose efficiency is comparable with that of an induction machine of similar size. However, the proposed machine in [13] would have an inferior electromagnetic performance compared to an equivalent double-stator permanent magnet machine due to the low flux-density and consequently low electromotive force and power generated in the former. Nevertheless, it should be noted that machines that are furnished with permanent magnets usually have higher cost implications than their magnetless counterparts due to high price of magnetic materials, especially the rare-earth ones.

Similarly, double-stator PM machines which utilize different kinds of magnets with special reference to a small amount of rare-earth magnet usage are proposed in [14] and [15]. The proposed machine in [14], which is suitable for various automobile driving situations, is capable of delivering reasonable electromagnetic torque with high flux-control flexibility compared to other traditional PM machines; however, it is associated with enormous fabrication issues owing to its multiple air-gap arrangement and a probable high cost outcome due to its increased mechanical weight. Though, a given machine size could be reduced and made more compact by employing appropriate stator, rotor and excitation materials. In addition, the investigated machine in [15] has enhanced field-weakening potential and thus an improved speed range, as well as a high tolerance to withstand demagnetization complications.

Research conducted in [16] shows that for a PM machine to yield an optimum performance, there should be a good synergy between its possible stator-rotor pole permutations and its optimal geometric parameters, such as the split ratio, length of PM, length and width of the modulating ring, etc.

Further, a detailed analysis on the influence of the design variables on the electromagnetic performance of PM machines in [17] confirms the fact that the overall output of a given PM machine would be a function of its optimal design variables, such as magnet size, stator and rotor pole selection, machine diameter, airgap size, number of turns, etc. The investigation in [17] is validated with experiments, with particular reference to the machine's mechanical strength, thermal and temperature effects, loss analysis, open circuit and on-load features, operational speed, etc. Basically, the output performance of any given machine would depend on both its geometric design sizes as well as its electric and magnetic loadings.

An analytical means of predicting the output torque of a single-stator switched-flux PM machine and possible determination of its geometric dimensions by inference using the Maxwell

stress tensor approach is presented in [18]. The proposed method in [18] shows a high likelihood of saving simulation time; nevertheless, the determination of its accuracy level is still underway.

A lot of magnetically-geared PM machine topologies are currently described in the literature though, more and more are still emerging owing to the machine's high torque and power competencies. In order to further increase the torque density of magnetically-geared PM machines, a new topology that has an additional modulating part is proposed in [19]. The enlarged torque production in [19] is achieved by the effective modulation of the airgap flux-density with the help of a supplementary modulator, which also tends to reduce or eliminate the possible leakage fluxes around the outer rotor configuration of the geared-machine.

The sections in this current paper are arranged as follows:

1. Introduction
2. Machine description and operating principle
3. Effect of model geometric variables
4. No-load characteristics
5. Load characteristics
6. Conclusion

A new type of double-stator permanent magnet machine capable of providing better electromagnetic performance than its single-stator type is proposed and analyzed in this present paper. The predicted 3D FEA flux density and field vector distributions displayed in Fig. 2 show that the investigated machine exhibits larger magnetic fields between the inner and outer stator teeth with the air-gap and the modulator regions inclusive, and would likely experience more saturation impacts around these regions.

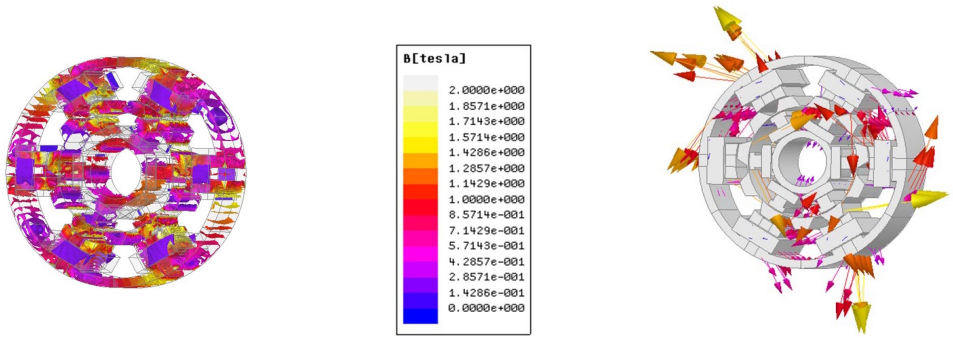

(a) (b) (c)

Fig. 2. Flux density and field vector contours, 3D FEA: flux density (a); scale (b); field vector (c)

2. Machine description and operating principle

The proposed machine has two different stators separated by a modulating ring, known as the rotor. Steel core components of the machine are made of M330-35A silicon material. Both the inner and outer stators are equipped with three-phase alternating current (AC) windings and are

connected in series for enhanced output. However, reliability of the machine could be improved by using the stators independently to ensure operational continuity; peradventure there is a fault in one sector of the machine, though, at a reduced operating capacity. It is worth mentioning that the number of turns in the inner and outer stators is shared respectively in the ratio of 1:2, due to different sizes of the slot areas and in order to maintain the same level of current density in these parts. The spoke arrangement of the PMs enhances the output torque of the machine by concentrating the fluxes towards the air-gap. It should be noted that the geometric variables of the machine are realized with the help of an intrinsic genetic algorithm (GA) procedure that is domiciled in the MAXWELL software, used under constant copper loss conditions.

The choice of geometrical data is based on the research models presented in [5] and [6]; where the global optimization of the models is undertaken using the intrinsic genetic algorithm process of the adopted software; with initial constraints selected between feasible maximum and minimum geometric lengths and ratios, while the sole objective is to attain the largest possible average torque. It should be noted that the inner stator structure of the proposed machine is entirely different from the ones in [5] and [6]; though, it is similar to that of the double-stator switched reluctance machine (DSSRM) presented in [20]. Nevertheless, a DSSRM usually has inferior torque density compared to that of permanent magnet machines. The proposed machine enjoys two operating principles i.e. the flux-switching and magnetic-gearing principles. The flux-switching principle fundamentally involves the capability of the machine to produce bipolar flux linkage and induced-EMF outlines by reversing its magnetic field path in half the electric period. Similarly, the magnetic-gearing principle primarily involves the modulation and synchronization of the combined active air-gap field harmonics generated by both the magnets and the windings (as applicable in this case), in order to produce the needed electromagnetic torque.

3. Effect of model geometric variables

Machine geometric variables are important elements in determining the output of a given electric machine; therefore, knowledge of its optimal values is paramount in order to realize the best performance from the machine. The static torque waveforms of the proposed machine under different load conditions are depicted in Fig. 3(a). It is shown that the magnitudes of static torques are dependent on the supplied currents i.e. the higher the input current, the larger the static torque and vice-versa. Although, there is a little difference between the compared 2D FEA and 3D FEA results at a current rating of 5 A; there is about a 13% static torque difference between the predicted 2D FEA and 3D FEA results at 15 A, owing to the influence of end windings coupled with the short stack length of the analyzed machine. Basically, the static torque waveform is symmetrical to the rotor angular positions.

Figure 3(b) shows the variation of output torque, induced-EMF, and flux linkage with the split ratio. An optimum split ratio of about 0.7 is obtained in Fig. 3(b). It is worth noting that a smaller value of the split ratio would yield a lower electromagnetic performance owing to its direct relationship with the overall machine size. Meanwhile, a larger value of the split ratio would reduce the length of the magnet in the outer stator as well as the available slot area for the excitation sources; hence, a corresponding adverse effect on the resultant machine's output performance will ensue. The split ratio, S_r, is given as the ratio of the rotor active airgap length

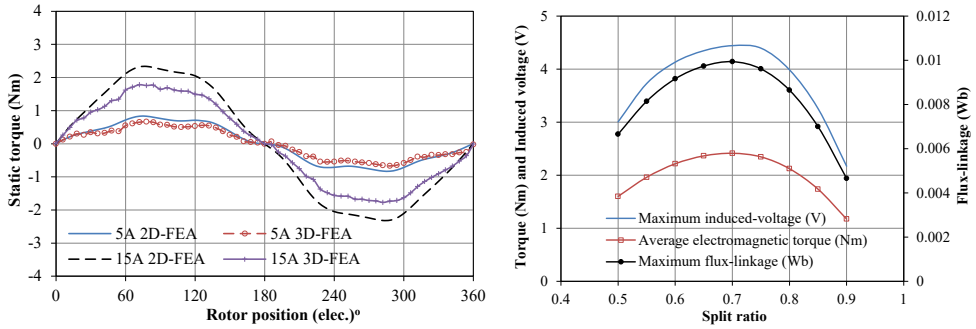

(a) (b)

Fig. 3. Comparison: static torque versus rotor position (a); torque, EMF, flux linkage versus split ratio (b)

to the length of outer stator radius, and it is expressed in (1). Similarly, the electrical frequency, f_r, of the developed machine is given in (2).

$$S_r = \frac{L_{rt}}{L_{st}}, \tag{1}$$

$$f_r = \frac{R_p N}{60}, \tag{2}$$

where: L_{rt} and L_{st} are the lengths of the rotor airgap and the outer stator, R_p is the rotor pole number, and N is the rotor speed (rpm).

Also, variation of the machine's output performances with PM thickness is depicted in Fig. 4(a). It could be inferred that the optimum value of the PM thickness is about 5 mm. Again, a smaller value of the PM size will result in a reduced amount of flux linkage contribution from the magnets while the oversized value of the PM thickness would negatively affect the conductor spaces; hence, a need for an ideal compromise between the stated PM thickness limits. Similarly, the variation of output torque, electromotive force and flux linkage with rotor radial thickness is

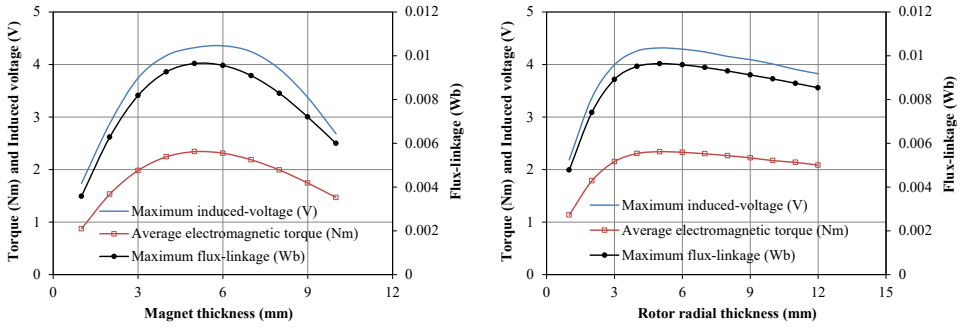

(a) (b)

Fig. 4. 2D FEA variation of torque, EMF, and flux linkage: PM thickness (a); rotor radial thickness (b)

presented in Fig. 4(b). It is shown that the optimum value of the rotor radial thickness is about 5 mm. Note also that a thinner size of the rotor radial thickness would give rise to an increase of easily saturated parts, while an enlarged rotor radial thickness would increase the level of leakage fluxes between both stators; thus, both extreme scenarios would lead to reduced machine performances, as observed in Fig. 4(b).

Further, variations of both the inner stator tooth-width and outer stator back-iron size are displayed in Fig. 5. Smaller sizes of these geometric parameters would escalate the saturation circumstances of these parts and consequently lead to reduced output. Additionally, when the sizes of the above mentioned two parameters are in excess; then, the available slot areas for the excitation sources would be hampered and subsequently affect the amplitudes of generated flux linkage, EMF and electromagnetic torque. Moreover, sensitivity of the outer stator yoke thickness to the machine performances is fairly constant beyond its optimum value of about 3.5 mm, as shown in Fig. 5(b), possibly due to saturation effects of the armature reaction. Furthermore, variations of the rotor inner iron-width/pitch ratio and rotor outer iron-width/pitch ratio are displayed in Fig. 6(a) and 6(b), respectively. The respective optimal values of the said geometric parameters

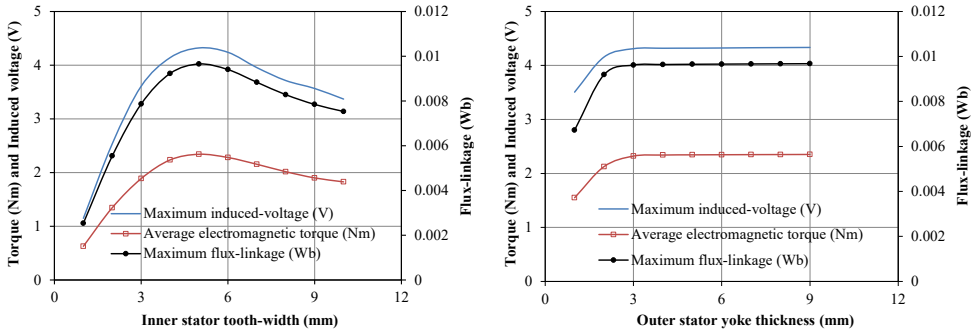

(a) (b)

Fig. 5. Variation of torque, EMF, and flux linkage: inner stator tooth-width (a); stator yoke thickness (b)

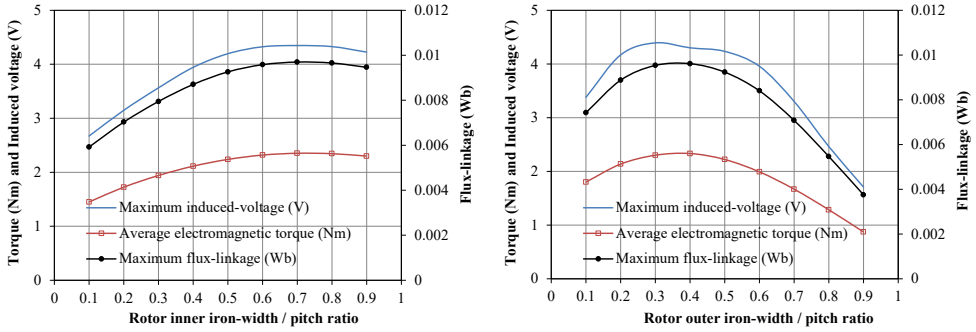

(a) (b)

Fig. 6. 2D FEA variation of torque, EMF, and flux linkage: rotor inner iron width/pitch ratio (a); rotor iron width/pitch ratio (b)

are 0.7 and 0.4; albeit, with a little perturbation on the resultant optimum induced-EMF value, owing to harmonic effect as a result of the high sensitivity of induced-voltage to harmonic issues. The geometric shape of a segmented rotor is vital in determining the overall performance of an electric machine as proved in [20]; the aforementioned shape is obtained by applying a proper optimization approach.

4. No-load characteristics

The coil-flux linkage of the proposed machine is given in Fig. 7. It is shown that the waveforms are sinusoidal and symmetrical in shape. Moreover, the outer stator produces more flux linkage than the inner stator because the total windings per phase are allocated based on the ratio of the outer stator to inner stator slot areas, which is 2:1 in this case. The peak-to-peak values of the conductor flux linkages in separate stators are 6.34 mWb and 3.30 mWb, respectively, with a total of 9.63 mWb contribution from both stators. Further, Fig. 8 shows the waveforms and harmonic spectra of induced-electromotive force in the conductors. Again, the larger contribution of EMF is made by the outer stator windings. Though the EMF waveforms are not completely sinusoidal; however, they are symmetrical along the measured range of angular positions.

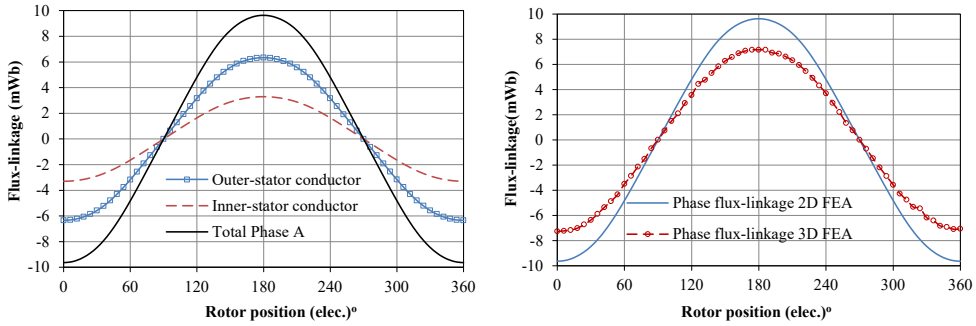

(a) (b)

Fig. 7. Comparison of flux linkage, 2D FEA: waveforms (a); phase flux linkage (b)

Similarly, the predicted 2D FEA and 3D FEA flux linkage waveforms in Phase A of the developed machine are presented in Fig. 7 with a magnitude of 9.63 mWb and 7.16 mWb, respectively. Again, the phase waveforms are absolutely symmetrical to the rotor angular positions. The noticeable difference in the compared flux-linkage results is due to the end winding effect. More importantly, there is a slight 5^{th} order harmonic content shown in the spectra of Fig. 8b. This may likely introduce torque ripple and cogging torque effects in the machine, as highlighted in [21]. The FEA predicted peak-to-peak coil-EMF values are 2.83 V and 1.47 V in the outer stator and inner stator, respectively.

A comparison of the cogging torques shown in Fig. 9 reveals that the proposed double-stator permanent magnet (DSPM) machine has lower cogging torque than its equivalent single-stator counterpart; this is a desirable quality in favour of the proposed machine for efficient control of

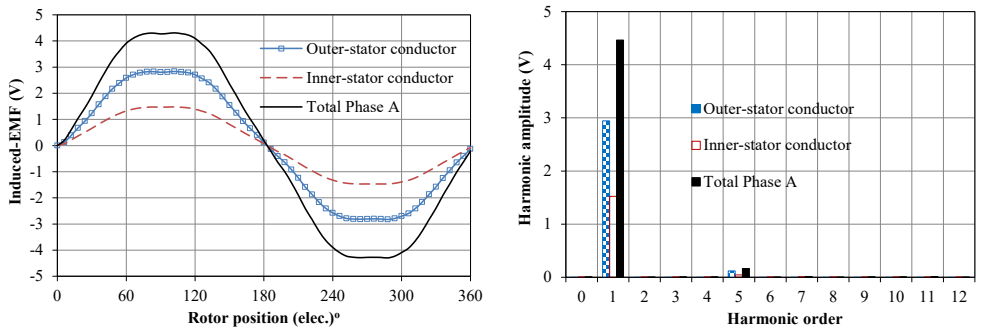

(a) (b)

Fig. 8. Comparison of induced-electromotive force at 400 rpm, 2D FEA: waveforms (a); FFT spectra (b)

electric machines. Note also that the estimated cogging torque amplitude of the proposed machine is less than 2% (percent) of its output electromagnetic torque. In general, the unavoidable cogging torque defect would be insignificant in the overall output torque and thus, can be compensated by the enormous resultant electromagnetic torque.

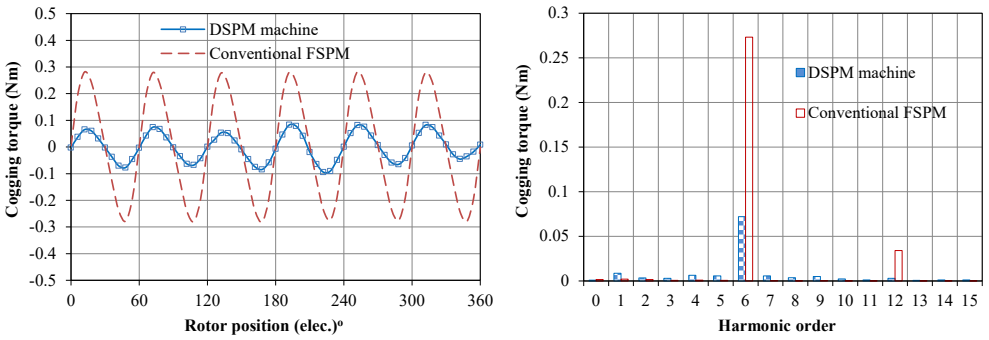

(a) (b)

Fig. 9. Comparison of cogging torque, 2D FEA: waveforms (a); FFT spectra (b)

5. Load characteristics

Electromagnetic torque of the investigate machines is compared in Fig. 10. The proposed machine has a fast Fourier Transform (FFT) torque value of 4.11 Nm while the traditional FSPM machine has a 3.56 Nm FFT torque value under a constant copper loss condition.

Meanwhile, the minor sixth order harmonic components in Fig. 10(b) imply that there could be a little torque ripple effect on both machines. Similarly, the influence of saturation in terms of current density and copper loss loadings on the compared machines is shown in Fig. 11. The curves show that the proposed double-stator machine produces larger average torque; in addition,

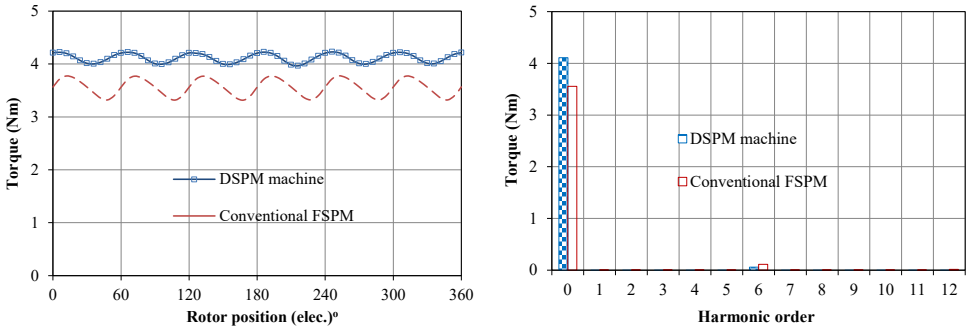

(a) (b)

Fig. 10. Comparison of output torque at copper loss of 30 W, 2D FEA: waveforms (a); FFT spectra (b)

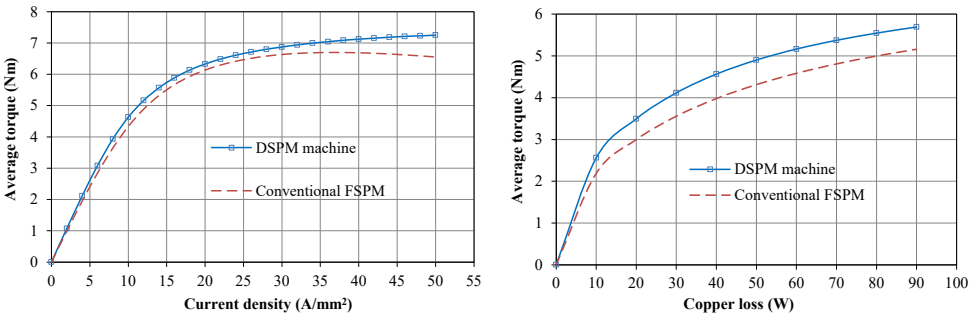

(a) (b)

Fig. 11. Comparison of average torque with: current density (a); torque versus copper loss (b)

it has a higher tolerance to saturation effects than the single-stator one. The output torque, T_{output}, of the proposed machine is given in (3). Figure 12 shows the comparison of losses in different parts of the investigated machines.

$$T_{\text{output}} = \frac{E_1 I_1 + E_2 I_2 + E_3 I_3}{\omega}, \tag{3}$$

where: ω is the rotational speed of the rotor, E_1, E_2, E_3 are the induced-voltages per phase, and I_1, I_2, I_3 are the corresponding applied phase currents.

It is observed that the proposed machine has both lower magnet eddy current loss and rotor core loss values, however with a high amount of stator core loss due to its dual stator configuration compared to a conventional FSPM machine. Overall, the proposed machine has better efficiency and lower total loss characteristics, which is desirable. The machines' total loss and maximum efficiency at 400 rpm and 15 A are listed in Table 1. Direct dependence of losses on thermal characteristics of a DSSRM is presented in [22], where it is demonstrated that the machine's general output and efficiency would be a function of its thermal content. Also, it is shown that different parts of the machine would exhibit varying temperature distributions to sections closer

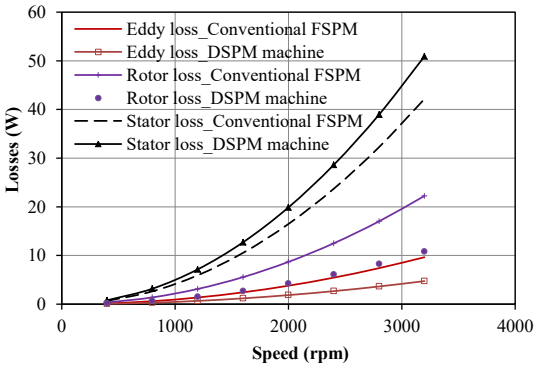

Fig. 12. Comparison of losses at 400 rpm and 15 A

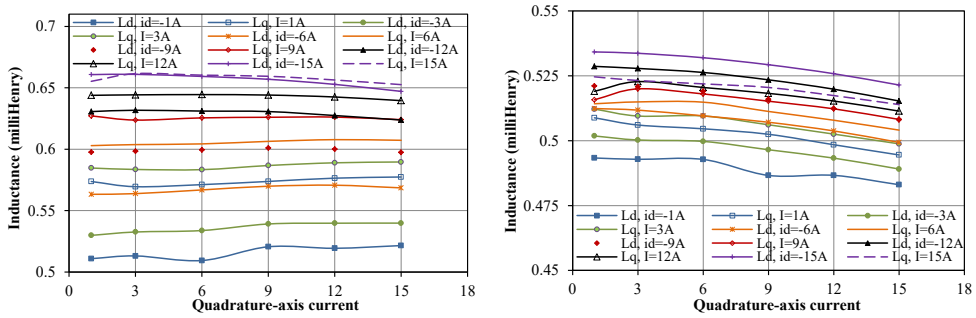

(a) (b)

Fig. 13. *D*-*q* inductance comparison at different currents: conventional FSPM (a); proposed DSPM (b)

to the airgap having the largest values, likely due to a high degree of energy conversion processes in this region. Moreover, it is verified in [23] that the rotor part would exhibit the largest amount of heat amongst various machine sections.

6. Conclusions

A new type of double-stator permanent magnet machine which is suited for direct-drive applications is developed and analyzed in this study. A comparative study between the 2D FEA and 3D FEA is also presented for enhanced result precision. The proposed machine has better electromagnetic performance than its corresponding single-stator counterpart. Additionally, the proposed machine has low cogging torque which is desirable for improved electric machine control purposes. Further, open-circuit waveforms of the proposed machine reveal that the flux linkage and induced-EMF waveforms are both sinusoidal and symmetrical, which are admirable for brushless AC electrical machine control applications. Furthermore, influence of design parameters on the average torque, induced-electromotive force and flux linkage of the developed double-stator

permanent magnet machine is also presented in this study. It is obvious that the performance of the machine is dependent on the optimal values of its geometry. Above all, the recommended machine is a promising candidate for high reliability and better fault-tolerance applications owing to its dual-stator architecture.

References

[1] Liu C., Chau K.T., Zhang Z., *Novel design of double-stator single-rotor magnetic-geared machines*, IEEE Transactions on Magnetics, vol. 48, no. 11, pp. 4180–4183 (2012), DOI: 10.1109/TMAG.2012.2201705.

[2] Salihu S.M., Misron N., Othman M.L., Hanamoto T., *Power density evaluation of a novel double-stator magnetic geared permanent magnet generator*, Progress In Electromagnetics Research B, vol. 80, no. 1, pp. 19–36 (2018), DOI: 10.2528/PIERB17102303.

[3] Wang Y., Cheng M., Chen M., Du Y., Chau K.T., *Design of high-torque-density double-stator permanent magnet brushless motors*, IET Electric Power Applications, vol. 5, no. 3, pp. 317–323 (2011), DOI: 10.1049/iet-epa.2010.0187.

[4] Reichert T., Nussbaumer T., Kolar J.W., *Split ratio optimization for high-torque PM motors considering global and local thermal limitations*, IEEE Transactions on Energy Conversion, vol. 28, no. 3, pp. 493–501 (2013), DOI: 10.1109/TEC.2013.2259169.

[5] Chen J.T., Zhu Z.Q., Iwasaki S., Deodhar R.P., *Influence of slot opening on optimal stator and rotor pole combination and electromagnetic performance of switched-flux PM brushless AC machines*, IEEE Transactions on Industry Applications, vol. 47, no. 4, pp. 1681–1691 (2011), DOI: 10.1109/TIA.2011.2155011.

[6] Awah C.C., Zhu Z.Q., *Influence of rotor pole number on electromagnetic performance of double-stator switched flux PM machines*, IEEE Vehicle Power and Propulsion Conference (VPPC), Hangzhou, China, pp. 1–6 (2016), DOI: 10.1109/VPPC.2016.7791709.

[7] Lin F., Qu R., Li D., *A novel fully superconducting geared machine*, IEEE Transactions on Applied Superconductivity, vol. 26, no. 7, pp. 1–5 (2016), DOI: 10.1109/TASC.2016.2594872.

[8] Huang X., Zhang K., Wu L., Fang Y., Lu Q., *Design of a dual-stator superconducting permanent magnet wind power generator with different rotor configuration*, IEEE Transactions on Magnetics, vol. 53 no. 6, pp. 1–4 (2017), DOI: 10.1109/TMAG.2017.2665600.

[9] Zhu X., Cheng M., Li X., Wang Y., *Topology analysis, design, and comparison of high temperature superconducting double stator machine with stationary seal*, IEEE Transactions on Applied Superconductivity, vol. 30, no. 1, pp. 1–10 (2020), DOI: 10.1109/TASC.2019.2914041.

[10] Shao L., Hua W., Li F., Soulard J., Zhu Z.Q., Wu Z., Cheng M., *A comparative study on nine- and twelve-phase flux-switching permanent-magnet wind power generators*, IEEE Transactions on Industry Applications, vol. 55, no. 4, pp. 3607–3616 (2019), DOI: 10.1109/TIA.2019.2910482.

[11] Shao L., Hua W., Soulard J., Zhu Z.Q., Wu Z., Cheng M., *Electromagnetic performance comparison between 12-phase switched flux and surface-mounted PM machines for direct-drive wind power generation*, IEEE Transactions on Industry Applications, vol. 56, no. 2, pp. 1408–1422 (2020), DOI: 10.1109/TIA.2020.2964527.

[12] Sun X., Zhu Z.Q., Wei F.R., *Voltage pulsation induced in DC field winding of different hybrid excitation switched flux machines*, IEEE Transactions on Industry Applications, vol. 57, no. 5, pp. 4815–4830 (2021), DOI: 10.1109/TIA.2021.3095432.

[13] Chen Y., Fu W., Weng X., *A concept of general flux-modulated electric machines based on a unified theory and its application to developing a novel doubly-fed dual-stator motor*, IEEE Transactions on Industrial Electronics, vol. 64, no. 12, pp. 9914–9923 (2017), DOI: 10.1109/TIE.2017.2733454.

[14] Chen Y., Ding Y., Li X., Zhu X., *Design and analysis of less-rare-earth double-stator modulated machine considering multioperation conditions*, IEEE Transactions on Applied Superconductivity, vol. 28, no. 3, pp. 1–5 (2018), DOI: 10.1109/TASC.2017.2786689.

[15] Chen Y., Zhuang J., Ding Y., Li X., *Optimal design and performance analysis of double stator multi-excitation flux-switching machine*, IEEE Transactions on Applied Superconductivity, vol. 29, no. 2 pp. 1–5 (2019), DOI: 10.1109/TASC.2019.2891899.

[16] Ren X., Li D., Qu R., Kong W., Han X., Pei T., *Analysis of spoke-type brushless dual-electrical-port dual-mechanical-port machine with decoupled windings*, IEEE Transactions on Industrial Electronics, vol. 66, no. 8, pp. 6128–6140 (2019), DOI: 10.1109/TIE.2018.2870395.

[17] Du G., Xu W., Zhu J., Huang N., *Effects of design parameters on the multiphysics performance of high-speed permanent magnet machines*, IEEE Transactions on Industrial Electronics, vol. 67, no. 5, pp. 3472–3483 (2020), DOI: 10.1109/TIE.2019.2922933.

[18] Kurtović H., Hahn I., *Calculation of active material's torque contributions for a flux switching machine*, IEEE Transactions on Magnetics, vol. 56, no. 2, pp. 1–4 (2020), DOI: 10.1109/TMAG.2019.2953377.

[19] Zhao H., Liu C., Song Z., Wang W., Lubin T., *A dual-modulator magnetic-geared machine for tidal-power generation*, IEEE Transactions on Magnetics, vol. 56, no. 8, pp. 1–7 (2020), DOI: 10.1109/TMAG.2020.3003788.

[20] Wang W., Luo M., Cosoroaba E., Fahimi B., Kiani M., *Rotor shape investigation and optimization of double Stator switched reluctance machine*, IEEE Transactions on Magnetics, vol. 51, no. 3, pp. 1–4 (2015), DOI: 10.1109/TMAG.2014.2356573.

[21] Zhao W., Kwon J., Wang X., Lipo T.A., Kwon B., *Optimal design of a spoke-type permanent magnet motor with phase-group concentrated-coil windings to minimize torque pulsations*, IEEE Transactions on Magnetics, vol. 53, no. 6, pp. 1–4 (2017), DOI: 10.1109/TMAG.2017.2664075.

[22] Arbab N., Wang W., Lin C., Hearron J., Fahimi B., *Thermal modeling and analysis of a double-stator switched reluctance motor*, IEEE Transactions on Energy Conversion, vol. 30, no. 3, pp. 1209–1217 (2015), DOI: 10.1109/TEC.2015.2424400.

[23] Maharjant L. *et al.*, *Comprehensive report on design and development of a 100-kW DSSRM*, IEEE Transactions on Transportation Electrification, vol. 4, no. 4, pp. 835–856 (2018), DOI: 10.1109/TTE.2018.2865665.